ACS Macro Letters

pubs.acs.org/macroletters Letter

Nanometer-Scale Water Dynamics in Nafion Polymer Electrolyte Membranes: Influence of Molecular Hydrophobicity and Water Content Revisited

Seung-Bo Saun, JiWon Kim, Ryeo Yun Hwang, Yeonho Ahn, Dukjoon Kim, Daniel K. Park, Soonchil Lee, and Oc Hee Han*

Cite This: *ACS Macro Lett.* 2020, 9, 1013−1018

Read Online

ACCESS | Metrics & More | Article Recommendations | Supporting Information

ABSTRACT: The ionic conductivity of polymer electrolyte membranes (PEMs) is an essential parameter for their device applications. In water-swollen PEMs, protons and other ions are transferred through hydrophilic channels of a few nanometers in diameter at most. Thus, optimizing the chemical and physical properties of the channels can enhance the conductivity of PEMs. However, the factors controlling the conductivity have not been completely clarified. Here, we report that measurements taken near the channel walls by a special nuclear magnetic resonance technique with ≤1 nm spatial resolution showed the largest water diffusivity when ∼80% of hydrophilic sulfonic acid groups were blocked, but the proton conductivity was low. The water diffusivity was much less affected by differences in water content. Our results provide a concept for changing the properties of PEMs and a challenge to implement the improved diffusivity in a way that enhances net ion conductivity.

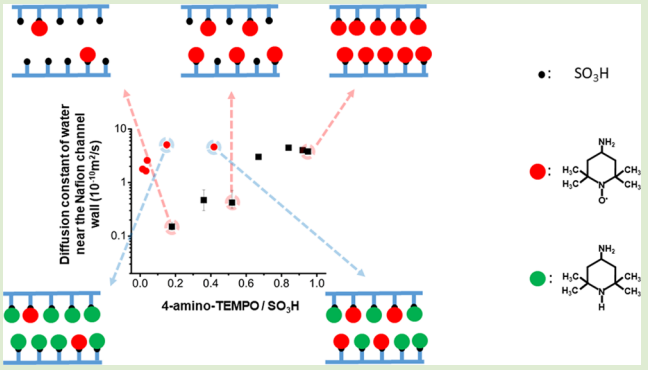

Polymer electrolyte membranes (PEMs) have been used as electrolytes in low-temperature fuel cells,[1] separators in redox batteries,[2] and actuators. How quickly and how many ions effectively move in PEMs are the main factors for determining the functional performance of these devices. Consequently, PEMs have been developed to have high ionic conductivity, and their mechanisms have been thoroughly investigated.[3−5] Nafion membranes are representative PEMs and have been used as references against which newly developed PEMs are compared. Nafion is composed of polytetrafluoroethylene (PTFE) backbones and perfluoroalkylether side chains that terminate in sulfonic acid (SO_3H) groups. The hydrophobic PTFE backbones provide mechanical strength to the PEM, and SO_3H groups in water-swollen PEM produce protons and assemble into hydrophilic channels through which water and protons can move.[6] Increasing the density of SO_3H groups in a PEM to make the hydrophilic channels dominant can enhance its ionic conductivity. However, this weakens the mechanical strength of the PEM and leads to greater variation of the PEM volume with the PEM water content. Thus, striking a balance between the mechanical properties and the ionic conductivity is essential in practical applications of PEMs.

Water plays an essential role not only in hydrophilic channel formation through interactions with ion-generating functional groups, such as SO_3H, but also in proton conduction through PEMs.[7] Water can be a carrier of protons through both the vehicle mechanism[8] and the Grotthuß mechanism.[9] The diffusivity and other dynamic properties of both the water and the protons being carried have been explored using pulsed field gradient-nuclear magnetic resonance (PFG-NMR) spectroscopy[10−13] and quasielastic neutron scattering (QENS).[14−16] Recently, an Overhauser dynamic nuclear polarization (ODNP)-NMR technique was shown to provide information about the dynamic properties of water in PEMs with ≤1 nm spatial resolution.[17] Consequently, ODNP-NMR has an advantage over PFG-NMR and QENS when differentiating the dynamics of water and protons near the inner surfaces of hydrophilic channels from those in the middle of the channels. Moreover, ODNP-NMR can measure mobility on a time scale from about 10 ps to 1 ns.[18] In contrast, PFG-NMR and QENS can measure dynamics on the order of 1 ms to 1 s and 1 ps to 1 μs, respectively.[10,19] Water and proton dynamics in PEMs are still under debate, including the water

Received: March 2, 2020
Accepted: June 17, 2020
Published: June 23, 2020

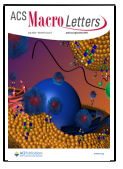

https://dx.doi.org/10.1021/acsmacrolett.0c00173
ACS Macro Lett. 2020, 9, 1013−1018

and proton diffusivities in Nafion membranes as measured by ODNP-NMR.[17] In ref 17, the diffusion coefficient of water (D_w) near the inner surfaces of Nafion hydrophilic channels was reported to be about 10000× larger than that of water in the middle of the channels. To probe the water dynamics near the inner channel surfaces, 4-amino-(2,2,6,6-tetramethylpiperidin-1-yl)oxyl (4-amino-TEMPO) has been employed as a spin-label compound with a stable unpaired electron. The NH_3^+ group of a 4-amino-TEMPO molecule is attracted to the SO_3^- groups of the side chains in the water-swollen Nafion through Coulomb interactions. The ion-generating SO_3H groups in PEMs play an important role in attracting water and promoting ionic conductivity.[20] Thus, blocking most of the SO_3H groups with 4-amino-TEMPO molecules is expected to result in the inner surfaces of the channels becoming hydrophobic, drastically altering the Nafion membrane properties.

In this work, 4-amino-TEMPO and 4-amino-(2,2,6,6-tetramethylpiperidine) (triacetonediamine, or TAD) are selected to control the hydrophobicity of the inner surfaces of the channels systematically and, in the case of 4-amino-TEMPO, to be a probe located near the channel surface at given concentrations. The dynamics of water near the Nafion channel walls is investigated by observing the dependence of D_w on the water content of the PEM and the channel surface concentration of 4-amino-TEMPO in the absence and presence of TAD. Systematic analyses of the ODNP-NMR data show the influence of the channel wall properties on the water and proton dynamics and predict D_w in the absence of 4-amino-TEMPO and TAD. In addition, a method to measure the amounts of spin-label compounds absorbed into PEMs is reported.

Dry, pretreated Nafion117 membrane sheets (35 mm × 6 mm × 0.178 mm) were immersed in purified water (12.5 MΩ cm, μ-Pure water system, Pure Power, Korea) for at least 1 h. Then, each swollen Nafion membrane sheet was transferred into 5 mL of 2.5, 5, 7.5, 10, 12.5, 15, or 20 mM 4-amino-TEMPO solutions, which were denoted as A2.5, A5, A7.5, A10, A12.5, A15, and A20, respectively. After at least 1.5 days, the Nafion membrane sheets were removed from the solutions. The remaining solutions were retained for the calculation of the average number of 4-amino-TEMPO molecules per SO_3H (α) in each Nafion membrane. The water content in each Nafion sample was also measured as the average number of water molecules per SO_3H (λ).

Using the same procedure, another set of Nafion membrane sheets was prepared and immersed in mixtures of 4-amino-TEMPO and TAD solutions. The sum of the 4-amino-TEMPO and TAD concentrations was 20 mM in each mixture. The 4-amino-TEMPO/TAD concentration ratios were 0:20, 1:7, 2:6, 3:5, 5:3, and 6:2, corresponding to 4-amino-TEMPO concentrations of 0, 2.5, 5, 7.5, 12.5, and 15 mM. The mixtures were denoted as M0, M2.5, M5, M7.5, M12.5, and M15, respectively. Nafion-A*n* and Nafion-M*m* represent the Nafion membrane sheets prepared with the corresponding A*n* and M*m* solutions. Detailed experimental procedures, including ODNP-NMR, electron paramagnetic resonance (EPR), and proton conductivity measurements are described in the Supporting Information (SI).

The α values were calculated using the EPR peak areas of the 5 mL solutions in which the Nafion sheets had been immersed. The difference between the 4-amino-TEMPO concenterations before and after Nafion-sheet immersion, as shown in Figure 1, provides the uptake amounts of 4-amino-TEMPO for the Nafion sheets.

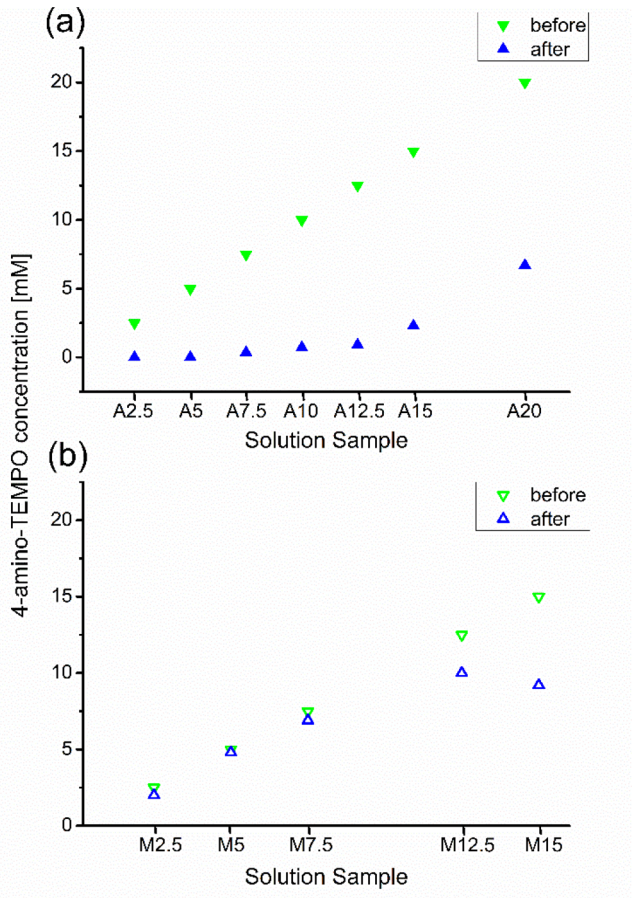

Figure 1. Plots of 4-amino-TEMPO concentrations in (a) 4-amino-TEMPO solutions, denoted A*n*, and (b) mixtures of 4-amino-TEMPO and TAD solutions, denoted M*m*, before (green inverse triangle) and after (blue triangle) immersion of a Nafion sheet (35 mm × 6 mm × 0.178 mm) for at least 1.5 days. The combined concentration of 4-amino-TEMPO and TAD was 20 mM in each M*m* solution. The error bars are not shown since they are smaller than the symbols representing the data.

The amount of SO_3H in each sheet was calculated to be 0.069 mmol using the weight of a dry Nafion sheet (0.076 ± 0.001 g) and the equivalent weight of Nafion117 (1100). The α value was calculated for each sample by dividing the 4-amino-TEMPO uptake by 0.069 mmol. The results are summarized in Table S1 in the SI, along with the lists of the concentration differences and 4-amino-TEMPO uptake amounts.

There was a greater uptake of 4-amino-TEMPO molecules by Nafion sheets immersed in A*n* than by those in M*m*, even when the solutions had the same initial concentrations of 4-amino-TEMPO. This indicates that the TAD molecules had higher affinity for SO_3H and bound to SO_3H more easily than the 4-amino-TEMPO molecules did despite their similar chemical structures (shown in Figure S1 in the SI). The line widths of the Nafion-M*m* samples are slightly broader than those of the Nafion-A*n* samples at the same effective α, as shown in Figure 2. This is likely due to the restricted motion of 4-amino-TEMPO when it is affected by neighboring TAD. Nevertheless, the split patterns of the EPR spectra of the

https://dx.doi.org/10.1021/acsmacrolett.0c00173
ACS Macro Lett. 2020, 9, 1013−1018

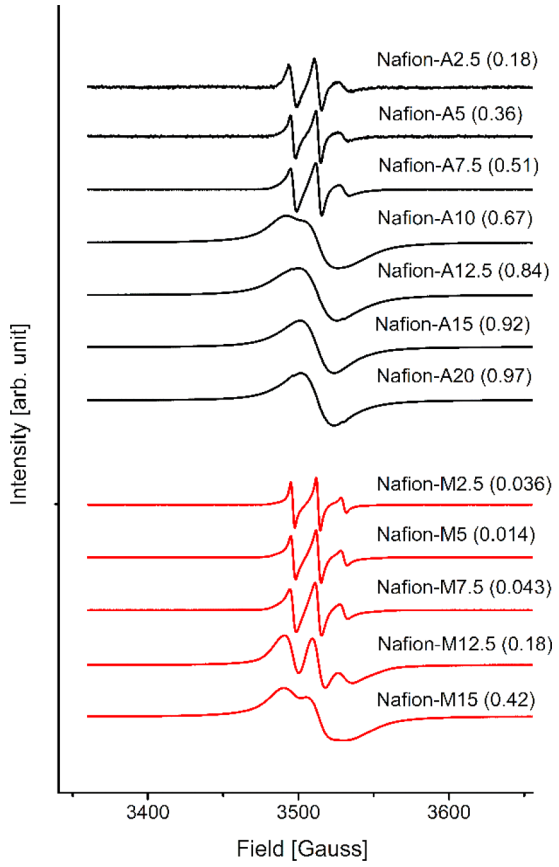

Figure 2. EPR spectra of the Nafion membranes. Nafion-A*n* and Nafion-M*m* are prepared in 4-amino-TEMPO solutions and mixtures of 4-amino-TEMPO and TAD solutions, respectively. The numbers in parentheses are the effective average numbers of 4-amino-TEMPO molecules per SO_3H group (α) in the Nafion membranes calculated with the EPR data used in Figure 1.

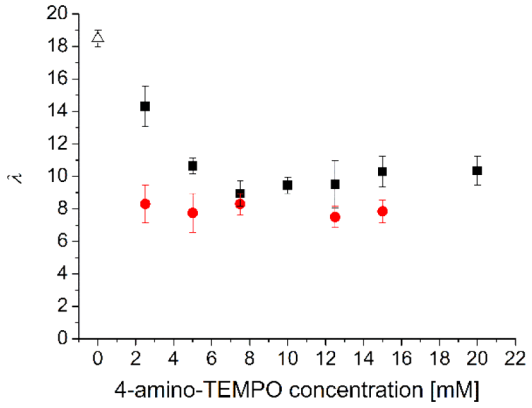

Figure 3. Water contents (λ) of Nafion samples prepared with 4-amino-TEMPO solutions (black filled square) and mixtures of 4-amino-TEMPO and TAD solutions (red filled circle) vs the initial concentrations of 4-amino-TEMPO in the solutions in which each Nafion sheet was immersed. Water content of water-swollen Nafion (black open triangle) is also shown for a reference.

Table 1. Diffusion Constants of Water (D_w) Near 4-Amino-TEMPO in Nafion Membrane at Different Water Contents (λ) and 4-Amino-TEMPO Amount (α), T_1, and $1 - E(p)$ under the Condition of lim $p \to \infty$

Nafion sample	D_w (10^{-10} m^2 s^{-1})	λ^a	α^b	T_1 (ms)	$1 - E(p)$ lim $p \to \infty$
Nafion-0				11	
Nafion-A2.5	0.15	14.3	0.18	3.5	0.082
Nafion-A5	0.47	10.7	0.36	9.2	0.13
Nafion-A7.5	0.42	9.0	0.51	2.6	0.95
Nafion-A10	3.0	9.5	0.67	0.49	17
Nafion-A12.5	4.5	9.5	0.84	0.5	31
Nafion-A15	4.0	10.3	0.92	0.41	27
Nafion-A20	3.8	10.4	0.97	0.39	23
Nafion-M0				58	
Nafion-M2.5	1.6	8.3	0.036	8.3	5.8
Nafion-M5	1.8	7.8	0.014	3.7	7.2
Nafiion-M7.5	2.6	8.3	0.043	1.8	14
Nafion-M12.5	5.1	7.5	0.18	0.73	38
Nafion-M15	4.6	7.9	0.42	0.39	34

[a]Average number of H_2O per SO_3H group. [b]Average number of 4-amino-TEMPO per SO_3H group.

Nafion-A*n* and Nafion-M*m* samples similarly merge to broad single patterns at higher effective α values. This line-broadening was confirmed to be mainly due to electron spin-electron spin dipole interaction when the distance between electron spins was $\lesssim$1 nm.[17] The hydrophilicity of the Nafion channel was expected to decrease as more 4-amino-TEMPO or TAD molecules were absorbed into the Nafion membranes. However, Figure 3 shows that the Nafion samples all had similar λ values. With the exception of Nafion A2.5 (λ = 14.3), each value was within the range of 7.5−10.7.

As described in detail in the ODNP-NMR spectroscopy section in the SI, the D_w values were obtained using $1 - E(p)$ values under the condition of lim $p \to \infty$ (Table 1), where $E(p)$ is the signal enhancement factor and p is the microwave power. The values were obtained by fitting the hyperbolic function with the $E(p)$ values[17,18] using the ^{1}H peak areas at various microwave powers. In Nafion-A*n* samples, the D_w values were larger when more SO_3H groups were blocked by 4-amino-TEMPO molecules, as shown in Table 1 and Figure 4. This indicates that more water was exposed to hydrophobic inner surfaces and that the reduction in water mobility due to water binding to SO_3H groups was mitigated.[17] The phenomenon of water molecules near SO_3H and fluorine showing reduced and increased mobility, respectively, is in good agreement with the simulated results reported by Gilois et al.[21] However, when the α values changed, the changing hydrophilicity of the channel surface possibly also caused variations in the other properties of the Nafion membranes, such as channel size and shape. Thus, it is desirable either to use samples with smaller α values to investigate the water dynamics near native Nafion channel walls or to compare the D_w values at a constant number of blocked SO_3H groups. In our work, Nafion-M*m* were all expected to have the same number of blocked SO_3H groups despite the variation in 4-amino-TEMPO concentrations because TAD molecules block SO_3H groups in a similar fashion to 4-amino-TEMPO molecules.

The D_w values of Nafion-M*m* were distinctly larger than the D_w values of the Nafion-A*n* with similar α values and were close to the D_w value of Nafion-A20, as shown in Figure 4. The reason that the Nafion-M*m* with α values below 0.1 had slightly smaller D_w values could be that fewer SO_3H groups were blocked in these samples than in the other Nafion-M*m* samples. The overall results indicate that both 4-amino-

https://dx.doi.org/10.1021/acsmacrolett.0c00173
ACS Macro Lett. 2020, 9, 1013−1018

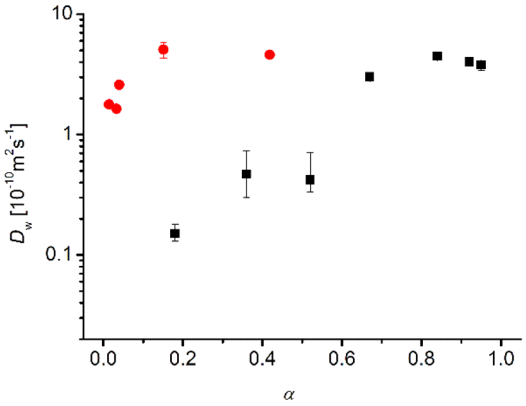

Figure 4. Plot of diffusion constants of water molecules (D_w) near Nafion channel walls versus average number of attached 4-amino-TEMPO per SO_3H (α) of Nafion samples. The raw data are listed in Table 1. Black filled squares represent Nafion-A*n* samples and red filled circles represent Nafion-M*m* samples.

TEMPO and TAD enhance the hydrophobicity of the channel walls in Nafion membranes and that water moves faster near the hydrophobic surfaces even on the nanometer scale. This faster movement of water over hydrophobic surfaces also supports the findings of previous reports.[17,22]

The D_w values of hydrated Nafion samples measured by PFG-NMR gradually increased about 20% as λ varied from 7 to 15.[23] These are spatially averaged D_w values because PFG-NMR does not spatially differentiate D_w values. This pattern might be interpreted as the larger λ inducing a larger D_w value mainly in the center region of the channel because the center region volume increased, while there was little change in the volume fraction at the channel wall surface. In contrast, the smallest D_w value near the channel walls in our Nafion-A*n* and Nafion-M*m* samples was of the sample with the largest λ value of 14.3. This indicates that the D_w variation due to differences in λ values was insufficient to undermine the D_w variation (up to ~340%) observed near the channel walls due to changes in α. This is likely because the local water content near the channel wall was not drastically changed by the variation in λ. This is consistent with the results of the simulation by Gilois et al. in that a subdiffusive phase existing near fluorine is independent of the water content.[21]

The D_w value of Nafion-A20 (3.8×10^{-10} m^2 s^{-1}), which had the largest α value of 0.97, was 8× larger than that of Nafion-A5 (0.47×10^{-10} m^2 s^{-1}), which had an α value of 0.36. This means that blocking SO_3H increased the D_w value near the channel walls 8-fold. The D_w value stabilized at α values at or above 0.8.

The water in a PEM can increase the internal pressure during fuel cell operation, which may degrade the durability of the PEM. Thus, techniques have been developed to reduce the amount of water in PEMs while obtaining a higher energy conversion efficiency through higher proton conductivity.[24] Blocking SO_3H by attaching 4-amino-TEMPO or TAD resulted in an increased effective equivalent weight. Therefore, α = 0.8 may be optimal for the balance between PEM durability and energy conversion efficiency.

The D_w value measured by PFG-NMR for a Nafion membrane with λ = 14 was reported as 6×10^{-10} m^2 s^{-1}.[23] This is close to the D_w value of a membrane with λ = 14 determined by QENS for the long-range diffusion (on the order of a few hundreds of picoseconds) influenced by the complex nanochannel system (4×10^{-10} m^2 s^{-1}).[25] In contrast, the D_w value measured by QENS for short-range diffusion (on the order of picoseconds) was 2×10^{-9} m^2 s^{-1},[25] which is very close to that of bulk water (2.3×10^{-9} m^2 s^{-1}).[11] Our smallest D_w value of 0.15×10^{-10} m^2 s^{-1}, which was from the Nafion-A2.5 sample with λ = 14.3, was much smaller than the D_w value for long-range diffusion (4×10^{-10} m^2 s^{-1}). The largest D_w value we obtained (5.1×10^{-10} m^2 s^{-1}) was between the D_w values obtained for long-range diffusion (4×10^{-10} m^2 s^{-1}) and by PFG-NMR (6×10^{-10} m^2 s^{-1}). This indicates that the range of the D_w values determined from ODNP-NMR data slightly differs from the ranges measured by other techniques, suggesting that the absolute D_w values might not be accurate.[17] However, the D_w values obtained from ODNP-NMR data clearly show an increasing tendency versus channel-wall hydrophobicity and site-specific detection ability with a spatial resolution of ≤1 nm, while PFG-NMR and QENS essentially detect bulk phenomena. This spatial resolution provides special opportunities for applications of ODNP-NMR techniques.

Since the diffusivity in Nafion 117 is isotropic before being pressure applied,[26] the measured diffusivity can represent the through-plane diffusivity as well. The in-plane proton conductivities were independently detected with impedance measurements (measuring net charge transfer); the results are summarized in Table 2. The data show that the diffusivity

Table 2. Proton Conductivity of Nafion Membranes

Nafion sample	conductivity (mS cm^{-1})
Nafion-0	31.9
Nafion-A2.5	13.0
Nafion-A20	3.62×10^{-2}
Nafion-M10	4.97×10^{-2}

measured does not correlate with the conductivity. This demonstrates that the measured diffusivity represents only the local properties of a small region near the inner hydrophobic surface and does not influence the conductivity throughout the PEM. Thus, for real-world applications, managing the morphological properties of the hydrophilic channels, such as tortuosity, is necessary to take advantage of the enhanced proton conductivity resulting from the increased surface hydrophobicity.

Our D_w values were highest at α = 0.8. The D_w variations due to α and λ were in opposite directions, and the former was much larger than the latter. Our results show that the surface hydrophobicity is a more important factor for controlling water mobility in nanopores and channels than the water content is. However, the much smaller proton conductivity of membranes with a high proportion of blocked SO_3H groups challenges us to use the enhanced nanoscopic diffusivity to improve the macroscopic conductivity by managing the morphology of the hydrophilic channels. The application of this ODNP-NMR technique can be expanded to other functional materials with nanopores or channels to investigate the interactions of the inner surfaces with water, protons, and, eventually, other chemical species. In addition, a simple EPR method to analyze the amounts of compounds with stable unpaired electrons absorbed into membranes was demonstrated. ODNP-NMR experiment designs using minimal amounts of spin-label compounds and minimizing the temperature perturbation in samples are in progress in our laboratory. In addition, isotherm

https://dx.doi.org/10.1021/acsmacrolett.0c00173
ACS Macro Lett. 2020, 9, 1013−1018

measurements of 4-amino-TEMPO and TAD by directly detecting them in membranes will be pursued by various methods.

■ ASSOCIATED CONTENT

Supporting Information

The Supporting Information is available free of charge at https://pubs.acs.org/doi/10.1021/acsmacrolett.0c00173.

Sample preparation, EPR methods, ODNP-NMR methods, ^{1}H ODNP-NMR spectra at different microwave power levels, Table S1 of 4-amino-TEMPO uptake and related data, and molecular structures of 4-amino-TEMPO and TAD (PDF)

■ AUTHOR INFORMATION

Corresponding Author

Oc Hee Han − *Western-Seoul Center, Korea Basic Science Institute, Seoul 03759, Republic of Korea; Department of Chemistry and Nano Science, Ewha Womans University, Seoul 03760, Republic of Korea; Graduate School of Analytical Science and Technology, Chungnam National University, Daejeon 34134, Republic of Korea;* orcid.org/0000-0003-1888-2323; Email: ohhan@kbsi.re.kr

Authors

Seung-Bo Saun − *Western-Seoul Center, Korea Basic Science Institute, Seoul 03759, Republic of Korea*

JiWon Kim − *Western-Seoul Center, Korea Basic Science Institute, Seoul 03759, Republic of Korea; Department of Chemistry and Nano Science, Ewha Womans University, Seoul 03760, Republic of Korea*

Ryeo Yun Hwang − *Western-Seoul Center, Korea Basic Science Institute, Seoul 03759, Republic of Korea; Graduate School of Analytical Science and Technology, Chungnam National University, Daejeon 34134, Republic of Korea*

Yeonho Ahn − *School of Chemical Engineering, Sungkyunkwan University, Suwon, Gyeonggi 16419, Republic of Korea*

Dukjoon Kim − *School of Chemical Engineering, Sungkyunkwan University, Suwon, Gyeonggi 16419, Republic of Korea;* orcid.org/0000-0001-6187-0737

Daniel K. Park − *Department of Physics, Korea Advanced Institute of Science and Technology, Daejeon 34141, Republic of Korea*

Soonchil Lee − *Department of Physics, Korea Advanced Institute of Science and Technology, Daejeon 34141, Republic of Korea*

Complete contact information is available at: https://pubs.acs.org/10.1021/acsmacrolett.0c00173

Notes

The authors declare no competing financial interest.

■ ACKNOWLEDGMENTS

This work was supported by the Grant (DRC-14-1-KBSI) of the National Research Council of Science and Technology in Korea to O.H.H., by Ministry of Science, the Grant (C39925) of the KBSI, and Technology Development Program to Solve Climate Changes (NRF-2018M1A2A2063349) through the National Research Foundation of Korea. We thank Dr. SangGap Lee at the Korea Basic Science Institute for the generous loan of an NMR console and informative discussion during the initial construction of a NMR system for the ODNP-NMR system.

■ REFERENCES

(1) Tang, H.; Pan, M.; Wang, F.; Shen, P. K.; Jiang, S. P. Highly Durable Proton Exchange Membranes for Low Temperature Fuel Cells. *J. Phys. Chem. B* **2007**, *111* (30), 8684−8690.

(2) Prifti, H.; Parasuraman, A.; Winardi, S.; Lim, T. M.; Skyllas-Kazacos, M. Membranes for Redox Flow Battery Applications. *Membranes* **2012**, *2*, 275−306.

(3) Steele, B. C. H.; Heinzel, A. Materials for Fuel-Cell Technologies. *Nature* **2001**, *414*, 345−351.

(4) Chen, D.; Wang, S.; Xiao, M.; Meng, Y. Synthesis and Characterization of Novel Sulfonated Poly(arylene thioether) Ionomers for Vanadium Redox Flow Battery Applications. *Energy Environ. Sci.* **2010**, *3*, 622−628.

(5) Kim, O.; Shin, T. J.; Park, M. J. Fast Low-Voltage Electroactive Actuators Using Nanostructured Polymer Electrolytes. *Nat. Commun.* **2013**, *4*, 1712.

(6) Gierke, T. D.; Munn, G. E.; Wilson, F. C. The Morphology in Nafion* Perfluorinated Membrane Products, as Determined by Wide- and Small-Angle X-Ray Studies. *J. Polym. Sci., Polym. Phys. Ed.* **1981**, *19*, 1687−1704.

(7) Kreuer, K. D. Proton Conductivity: Materials and Applications. *Chem. Mater.* **1996**, *8*, 610−641.

(8) Kreuer, K. D.; Rabenau, A.; Weppner, W. Vehicle Mechanism, A New Model for the Interpretation of the Conductivity of Fast Proton Conductors. *Angew. Chem., Int. Ed.* **1982**, *21* (3), 208−209.

(9) Howe, A. T.; Shilton, M. G. Studies of Layered Uranium (VI) Compounds. I. High Proton Conductivity in Polycrystalline Hydrogen Uranyl Phosphate Tetrahydrate. *J. Solid State Chem.* **1979**, *28*, 345−361.

(10) Zawodzinski, T. A., Jr; Neeman, M.; Sillerud, L. O.; Gottesfeld, S. Determination of Water Diffusion Coefficients in Perfluorosulfonate Ionomeric Membranes. *J. Phys. Chem.* **1991**, *95*, 6040−6044.

(11) Holz, M.; Heil, S. R.; Sacco, A. Temperature-Dependent Self-Diffusion Coefficients of Water and Six Selected Molecular Liquids for Calibration in Accurate ^{1}H NMR PFG Measurements. *Phys. Chem. Chem. Phys.* **2000**, *2*, 4740−4742.

(12) Li, J.; Park, J. K.; Moore, R. B.; Madsen, L. A. Linear Coupling of Alignment with Transport in a Polymer Electrolyte Membrane. *Nat. Mater.* **2011**, *10*, 507−511.

(13) Zhao, Q.; Majsztrik, P.; Benziger, J. Diffusion and Interfacial Transport of Water in Nafion. *J. Phys. Chem. B* **2011**, *115*, 2717−2727.

(14) Pivovar, A. M.; Pivovar, B. S. Dynamic Behavior of Water within a Polymer Electrolyte Fuel Cell Membrane at Low Hydration Levels. *J. Phys. Chem. B* **2005**, *109*, 785−793.

(15) Berrod, Q.; Lyonnard, S.; Guillermo, A.; Ollivier, J.; Frick, B.; Gebel, G. QENS Investigation of Proton Confined Motions in Hydrated Perfluorinated Sulfonic Membranes and Self-Assembled Surfactants. *EPJ Web Conf.* **2015**, *83*, 02002.

(16) Berrod, Q.; Hanot, S.; Guillermo, A.; Mossa, S.; Lyonnard, S. Water Sub-Diffusion in Membranes for Fuel Cells. *Sci. Rep.* **2017**, *7*, 8326.

(17) Song, J.; Han, O. H.; Han, S. Nanometer-Scale Water-and Proton-Diffusion Heterogeneities across Water Channels in Polymer Electrolyte Membranes. *Angew. Chem., Int. Ed.* **2015**, *54*, 3615−3620.

(18) Kausik, R.; Han, S. Ultrasensitive Detection of Interfacial Water Diffusion on Lipid Vesicle Surfaces at Molecular Length Scales. *J. Am. Chem. Soc.* **2009**, *131* (51), 18254−18256.

(19) Berrod, Q.; Lagrené, K.; Ollivier, J.; Zanotti, J.-M. Inelastic and Quasi-elastic Neutron Scattering. Application to Soft Matter. *EPJ Web Conf.* **2018**, *188*, 05001.

(20) Yang, C.; Srinivasan, S.; Bocarsly, A. B.; Tulyani, S.; Benzier, J. B. Comparison of Physical Properties and Fuel Cell Performance of Nafion and Zirconium Phosphate/Nafion Composite Membranes. *J. Membr. Sci.* **2004**, *237* (1-2), 145−161.

(21) Gilois, B.; Goujon, F.; Fleury, A.; Soldera, A.; Ghoufi, A. Water Nano-Diffusion Through the Nafion Fuel Cell Membrane. *J. Membr. Sci.* **2020**, *602*, 117958.

(22) Kim, H. N.; Hwang, R. Y.; Han, O. H. Behavior of Channel Water and CF_2H Side-Chain Terminal Groups in Swollen Nafion Polymer Electrolyte Membranes after Thermal Treatment. *ACS Macro Lett.* **2016**, *5*, 801−804.
(23) Tsushima, S.; Teranishi, K.; Hirai, S. Water Diffusion Measurement in Fuel-Cell SPE Membrane by NMR. *Energy* **2005**, *30*, 235−245.
(24) Chandan, A.; Hattenberger, M.; El-Kharouf, A.; Du, S.; Dhir, A.; Self, V.; Pollet, B. G.; Ingram, A.; Bujalski, W. High Temperature (HT) Polymer Electrolyte Membrane Fuel Cells (PEMFC)-A Review. *J. Power Sources* **2013**, *231*, 264−278.
(25) Perrin, J.-C.; Lyonnard, S.; Volino, F. Quasielastic Neutron Scattering Study of Water Dynamics in Hydrated Nafion Membranes. *J. Phys. Chem. C* **2007**, *111*, 3393−3404.
(26) Kim, S. H.; Mehmood, A.; Ahn, Y.; Kim, H.-S.; Ha, H. Y.; Kim, D.; Han, O. H. Proton Conductivity Improvement of Polymer Electrolyte Membrane Using Nano-Scale Explosion of Water in the Membrane. *J. Electroanal. Chem.* **2016**, *782*, 32−35.

https://dx.doi.org/10.1021/acsmacrolett.0c00173
ACS Macro Lett. 2020, 9, 1013−1018